Published in final edited form as:
Int J Biochem Cell Biol. 2013 June ; 45(6): 1051–1063. doi:10.1016/j.biocel.2013.02.015.

The Carboxyl Tail of Alpha-Actinin-4 Regulates Its Susceptibility to m-Calpain and thus Functions in Cell Migration and Spreading

Hanshuang Shao[1], **Tim Travers**[2], **Carlos Camacho**[2], and **Alan Wells**[1]

[1]Department of Pathology, University of Pittsburgh, Pittsburgh, PA 15261

[2]Department of Computational and Systems Biology, University of Pittsburgh, Pittsburgh, PA 15261

Abstract

Alpha-actinin-4 links the cytoskeleton to sites of adhesion and has been shown to be modulated to enable cell migration. Such focal adhesions must be labile to accomplish migration, with this detachment occurring at least in part via m-calpain activation (Glading et al., 2002, Glading et al., 2001, Xie et al., 1998). In this study, we report that alpha-actinin-4 is initially cleaved by m-calpain between tyrosine 13 and glycine. Removal of the first 13 amino acids does not affect alpha-actinin-4 binding to actin filaments and its localization within fibroblasts but drives cell migration with less persistence. Binding of phosphoinositides PI(4,5)P2, PI(3,4,5)P3 and PI(3,4)P2 to alpha-actinin-4, as well as binding of alpha-actinin-4 to actin filaments all inhibit m-calpain cleavage of ACTN4 between tyrosine 13 and glycine 14. Interestingly, the carboxyl terminus of alpha-actinin-4 including its calcium binding motifs, is inhibitory for a secondary cleavage of alpha-actinin-4 between lysine 283 and valine 284.The minimal length of inhibitory domain is mapped to the last 11 amino acids of alpha-actinin-4. The C-terminal tail of alpha-actinin-4 is essential for maintaining its normal actin binding activity and localization within cytoplasm and also its colocalization with actin in the lamellipodia of locomoting fibroblasts. Live cell imaging reveals that the 1–890 fragment fails to rescue neither the basal or growth factor-stimulated migration nor the revert the spread area of fibroblasts to the level of NR6WT. These findings suggest that the C-terminal tail of alpha-actinin-4 is essential for its function in cell migration and adhesion to substratum.

1. Introduction

Alpha-actinin 4 (ACTN4), originally identified as a novel isoform of alpha-actinin, belongs to a superfamily of actin crosslinking proteins; of the four isoforms, ACTN1 and ACTN4 are ubiquitously expressed in non-muscle cells (Honda et al., 1998, Otto, 1994). The ACTN4 isoform has been shown to play a crucial role in cell spreading and migration, and cancer invasion and metastasis (Honda, Yamada, 1998, Honda et al., 2005, Kikuchi et al., 2008, Quick and Skalli, 2010, Sen et al., 2009, Shao et al., 2010a, Yamamoto et al., 2009). Besides cross-linking actin filaments, ACTN4 is also involved in cell-cell and cell-extracellular matrix junctions by linking the filaments of the cytoskeleton to the inner face of the substratum contacts, whereas the ACTN1 isoform is considered mainly to bridge

Address correspondence to: Alan Wells, MD DMSc, 713 Scaife, Dept of Pathology, University of Pittsburgh, Pittsburgh, PA 15261, FAX: 412-647-8567, wellsa@upmc.edu.

between actin filaments to form or stabilize stress fibers. Thus, understanding the regulatory control of ACTN4 would highlight the dynamic control of actin cytoskeleton plasticity and the interplay between cell shape, adhesion strength, and transcellular contractility critical for locomotion.

Recent dissection of the structure of the functionally active anti-parallel ACTN4 homodimers suggests modes of regulation (Lee et al., 2008). ACTN4 forms an anti-parallel, dumbbell-shaped homodimer through the interaction of actin binding domain (ABD) head of one molecule and the carboxyl terminal calcium binding motifs of another molecule as well as the interaction between two central rod domains that align in an opposite direction (Blanchard et al., 1989, Davison and Critchley, 1988, Otey and Carpen, 2004, Ylanne, Scheffzek, 2001). Although the crystal structures of ABD and central rod domains of actinin have been recently resolved, the intact actinin protein has not been crystallized, due to its large size and the flexible N-terminus (Borrego-Diaz et al., 2006, Ylanne, Scheffzek, 2001). Thus, the mechanistic aspects of the various domains and modifications such as phosphorylation remain speculative. Our previous study showed that epidermal growth factor (EGF) significantly enhanced the phosphorylation of ACTN4 at tyrosine 4 and 31 resulting in a decrease in its actin binding activity (Shao et al., 2010b). Recently, we have developed a structural model which shows a ternary complex being formed via the interaction among three domains of the N-terminal ABD and its adjacent helical neck region of one monomer and the C-terminal CaM-like motif of the opposite antiparallel monomer and this model is verified by an *in vitro* experimental actin binding assay (Travers et al., 2013). Other than this novel finding and the role in binding of calcium, other possible functions of the ACTN4 C-terminal still remain largely unknown.

Recently, ACTN1 has been shown to be cleaved by m-calpain in the presence of PI(3,4,5)P3 even thought actinins were previously thought not to be substrates of m-calpain (Sprague et al., 2008). m-Calpain, (the CAPN2-CAPNS1 dimer) is a ubiquitous intracellular limited protease that plays a crucial role in cell motility (Dourdin et al., 2001, Glading et al., 2002). Our previous studies showed that m-calpain is involved in cell migration by mediating the detachment at the rear of motile fibroblasts upon stimulation of EGF (Chou et al., 2002, Leloup et al., 2010, Shao et al., 2006). Although the amino acid identity between human ACTN1 and ACTN4 is 86 percent, it is not clear if ACTN4 can be cleaved by m-calpain as the target sequence is structurally constrained (Ono and Sorimachi, 2012, Tompa et al., 2004). Further, as ACTN4 crossbridges to the actin cytoskeleton, the function of proteolytic cleavage would be distinct. In the present study we find that m-calpain cleaves intact ACTN4 initially between Tyr13 and Gly14. The carboxyl-tail of ACTN4 functions as an inhibitory domain of a secondary m-calpain cleavage between Lys283 and Val284. The minimal length required to prevent cleavage of ACTN4 between Lys283 and Val284 by m-calpain is mapped to the last 11 amino acids. Removal of more than 11 amino acids from the carboxyl-tail of ACTN4 significantly impairs cell migration and spreading.

2. Materials and Methods

2.1. Antibodies

GFP antibody was purchased from Life Technologies Invitrogen (Grand Island, NY). Anti-phosphotyrosine, monoclonal anti-vinculin, G-actin, Mowiol 4–88, calcium ionophore A23187were purchased from Sigma (St. Louis, MO). Monoclonal anti phosphor-Tyr (P-Tyr-100) was purchased from Cell Signaling Technology (Danvers, MA). Rhodamine phalloidin and ER red tracker were purchased from Life Technologies Invitrogen Molecular Probes (Grand Island, NY). HisTrapTM HP columns were purchased from GE Healthcare Biosciences (Piscataway, NJ). ProteoExtract® Cytoskeleton Enrichment and Isolation Kit were purchased from EMD Millipore (Billerica, MA).

2.2. Cell lines

NR6WT murine fibroblasts expressing the human EGFR were cultured in Alpha-MEM (Cellgro, Lawrence, KS) with 7.5% fetal bovine serum, 1× nonessential amino acids, 1× sodium pyruvate, 2 mM L-glutamine, 1× streptomycin/penicillin (Invitrogen) supplemented with 350 μg/ml G418 (EMD, Gibbstown, NJ). NR6WT ACTN4 KD fibroblasts grow in same media as NR6WT in addition of 2.5 μg/ml puromycin.

2.3. Mutagenesis, expression and purification of ACTN4

All mutations and purification of ACTN4 were performed as described previously (Shao, Wu, 2010b). The secondary structure of full length human WT ACTN4 expressed and purified from *E.coli.* was analyzed using circular dichroism by Northwestern University Keck Physics Facility (Evaston, IL).

2.4. m-Calpain-mediated cleavage

ACTN4, ACTN1 and their mutants (1μg) expressed and purified from *E.coli* were incubated with indicated amounts of m-calpain at 30°C for 1h. Reactions were terminated by the addition of 1/5 volume of 5× SDS sample buffer and boiled for 3 min prior to loading on SDS-PAGE for separation of protein bands. Protein bands were visualized by either Coomassie staining or immunoblotting or both. For the effects of PIPs on ACTN4 cleavage by m-calpain, PI(4,5)P2,PI(3,4,5)P3 and PI(3,4)P2 (each 50 μM), respectively were preincubated with ACTN4 at room temperature for 30 min prior to the addition of m-calpain.

2.5. N-terminal protein sequencing

After m-calpain cleavage and electrophoresis, proteins were transferred to polyvinylidene difluoride PVDF membrane and stained with Coomassie G250 for 1 minute and then destained till membrane background is light. Target protein bands were excised and their sequences of the first five N-terminal amino acids were identified by the Iowa State University protein facility (Ames, IA).

2.6. F-actin filament sedimentation assays

Actin filament sedimentation assays were performed as described previously (Shao et al., 2010b).

2.7. Isolation of cellular cytoskeleton

Isolation of cellular cytoskeleton was performed following the manufacture instructions. In brief, confluent and transiently transfected cells gently washed with cold PBS were incubated with 1× cellular extraction buffer on ice for 90 seconds followed by pipetting solution up and down for several times. Then the solution was collected as soluble cellular compartment (S). The rest compartment still residing on petri dish was gently washed once with 1× cytoskeleton wash buffer and further incubated with nuclear extraction buffer on ice for 10 min. The solution was aspirated and the cytoskeleton remaining on petri dish was washed twice with cytoskeleton wash buffer followed by extraction with cytoskeleton solubilization buffer (C). The proteins of both soluble compartment (S) and cytoskeleton (C) were separated by SDS-PAG electrophoresis and immunoblotted using appropriate antibodies.

2.8. Cell spreading assay

Murine fibroblasts NR6WT in which ACTN4 was stably knocked down by shRNA (ACTN4 KD) were transiently transfected with either WT or mutant human ACTN4 plasmid tagged

with eGFP for 16–24h. Cell spreading assay was performed as described previously (Shao et al., 2010a) with the enumeration of the cross-sectional area presented by the cell.

2.9. Continuous cell tracking

For cell tracking experiments, NR6WT ACTN4 KD fibroblasts transiently transfected with either WT or mutant human ACTN4 plasmids tagged with eGFP for 16–24h prior to experiments were visualized every 10min for duration of 16h under Nikon live cell fluorescent microscopy. The velocity of the cells was determined using MetaMorph software.

3. Results

3.1.m-Calpain cleaves intact ACTN4 between Tyrosine 13 and Glycine 14

m-Calpain modulates growth factor induced motility by cleaving intracellular structural proteins that link adhesion sites to the actin cytoskeleton (Glading et al., 2002). The remaining fragments may then act as dominant effectors, such as in the case of talin, where the adhesion- and F-actin-interacting domains are separated but each domain is left intact and functional (Schoenwaelder et al., 1997). As alpha-actinin-4 (ACTN4) links the cytoskeleton to focal adhesion sites in a dynamically regulated fashion (Michaud et al., 2009, Shao et al., 2010a) and is similarly comprised of independently interacting domains (Lee et al., 2008, Sjoblom et al., 2008, Travers et al., 2013, Ylanne et al., 2001), we queried whether ACTN4 was also a target for m-calpain.

To determine whether m-calpain cleaves ACTN4, a 6×His-tagged clone was expressed in *E. coli*, and soluble ACTN4 was purified and then incubated with recombinant rat m-calpain in the presence of 1 mM calcium at 30°C for an hour. Interestingly, the full length (FL) ACTN4 was cleaved at its proximal terminal with m-calpain in a dose-dependent manner (Figure 1A Coomassie stained gel). The product of ACTN4 cleaved with m-calpain, a ~100 kD fragment that is the bottom band of a doublet on SDS-PAGE was resistant to further cleavage with m-calpain. Since only a tiny fragment was removed after m-calpain cleavage, the cleavage site should be localized at either amino acidic or carboxyl terminus. To identify the localization of m-calpain cleavage, we performed an immunoblotting using an ACTN4 antibody that specifically recognizes its N-terminal amino acid 2–11. As shown in Figure 1A middle panel, the signal decreases with increasing concentrations of m-calpain but the signal of immunoblotting bands using another monoclonal ACTN4 antibody (H-51 raised from the C-terminus of ACTN4) mainly remains unchanged indicating the m-calpain cleavage of ACTN4 occurs at its N-terminus. To exclude the possibility that m-calpain cleavage of ACTN4 was due to incorrect protein folding in *E.coli.*, we analyzed the secondary structure of bacterially-expressed full length WT ACTN4 using circular dichroism. We found that WT ACTN4 contains alpha-helixes and beta-sheets suggesting that WT ACTN4 was correctly folded (Figure 1B). The secondary structure ratios based on the CD spectra are 0.626 (helixes) : 0.063 (sheets) : 0.115 (turns) : 0.194 (coils) that are very similar to 0.65 (helixes) : 0.01 (sheets) : 0.14 (turns) : 0.20 (coils) indicated from structural models of full-length WT ACTN4 (incorporating experimental structures of ABD, spcetrin rods, and CaM). Furthermore, SEC-MALS-QELS data also related that about 70% of the WT ACTN4 was a dimer with apparent MW of around 220 KDa and the hydrodyamic radius of this dimer was approximately 8.8nm. These findings further support the contention that this species is properly folded. ACTN4-eGFP immunoprecipitated from fibroblasts were similarly cleaved by m-calpain although the eGFP was also removed by m-calpain (Figure 1C), further indicating that the susceptibility of ACTN4 to m-calpain occurs in eukaryotic-folded protein.

In order to determine the cleavage site of ACTN4 by m-calpain, N-terminal sequence analysis of the large truncated ACTN4 fragment was performed and revealed that m-calpain cleaved ACTN4 between tyrosine 13 (Tyr13) and Glycine 14 (Gly14), a different cleavage site to ACTN1 (Sprague, Fraley, 2008). The cleavage of ACTN4 by m-calpain between Tyr13 and Gly14 was further confirmed by a mutant Q12D, which was significantly resistant to m-calpain *in vitro* and *in vivo* (Figure 1D and 1E). In order to directly detect the cleavage of ACTN4 by m-calpain between Tyr13 and Gly14 within cells, we treated the NR6WT ACTN4 KD fibroblasts in which endogenous ACTN4 was significantly and stably abrogated using murine species specific ACTN4 shRNA (Figure 1F). Full-length (FL) human WT ACTN4-eGFP was transiently expressed and the cells treated with the calcium ionophore A23187, a common agent to enhance the activity of calpain *in vivo* (Sprague, Fraley, 2008). An antibody specific to the N-terminus 11 amino acids demonstrated a decrease in FL WT ACTN4-eGFP level suggesting that ACTN4 is a substrate of calpain within cells (Figure 1G).

As K255E, a native mutant of ACTN4 found in patients suffering from a familial kidney disease, focal and segmental glomerulosclerosis presents an increased actin binding activity and abnormal cellular localization (Weins et al., 2007), we asked if this mutation affects its susceptibility to m-calpain. Surprisingly, K255E was digested by m-calpain in a similar pattern as WT ACTN4, whereas another mutant Y265E, a mimic of phosphorylated ACTN4 at Y265 that also bound actin filaments extremely stably is much more sensitive to m-calpain cleavage which resulted in additional three major protein bands that were not seen in WT ACTN4 and K255E (Figure 1H). This result suggested that the susceptibility of K255E to m-calpain between Y13 and G14 is not involved in the pathogenesis of the resultant glomerulosclerosis.

3.2. Removal of the first 13 amino acids does not affect the actin binding activity of ACTN4 but decreases persistence of fibroblast migration

Our previous study showed that EGF-mediated phosphorylation of ACTN4 occurred at tyrosine 4 (the major site) and tyrosine 31 (a minor site) (Shao et al., 2010b) resulting in a decrease in its actin binding activity. As tyrosine 4 resides within the removed fragment of ACTN4 cleaved with m-calpain, we expressed and purified the soluble ACTN4 fragment 14–911 for analysis of its actin binding activity. As shown in Figure 2A, 14–911 bound actin similar with FL WT ACTN4 suggesting that ACTN4 proteolysis with m-calpain did not cause a change in its actin binding activity. To exclude the possibility of protein expressed in *E.coli* was not correctly folded, we isolated cellular cytoskeleton using a cytoskeleton enrichment and isolation kit for detecting the actin binding/bundling activity of FL WT ACTN4 and truncated fragment 14–911. As shown in Figure 2B, the percent of FL WT ACTN4-eGFP remaining in cytoskeleton is very similar with 14–911-eGFP even though the total expression level of 14–911-eGFP was lower than FL WT ACTN4-eGFP. In order to determine if the removal of the first 13 amino acids affects the function of ACTN4 in cell migration, we continually tracked NR6WT ACTN4 KD in which either FL WT ACTN4-eGFP or 14–911 ACTN4-eGFP was transiently expressed in normal growth media. Figure 2C showed that 14–911 ACTN4-eGFP restored cell migration of ACTN4 KD fibroblasts to FL WT ACTN4-eGFP level but cells expressing 14–911 ACTN4-eGFP migrated with less persistence comparing to FL WT ACTN4-eGFP expressed cells (Figure 2D) although 14–911 ACTN4-eGFP and FL ACTN4-eGFP localized similarly within NR6WT ACTN4 KD fibroblasts (Figure 2E). This result suggested that the removal of the first 13 amino acids did not disturb the tri-complex consisting of actin binding domain, neck and calcium binding motifs which was suggested by simulation and experimentally tested to be essential for maintaining normal actin binding activity of ACTN4 (Travers et al., 2013) although how 14–911 ACTN4 affects the persistence of cell migration remains unclear.

3.3. Phosphoinositides decrease the susceptibility of ACTN4 to m-calpain cleavage

Phosphoinositides in the membrane help stabilize ACTN4 bridging from the adhesion plaque to the cytoskeleton. These moieties also have been shown to enhance the susceptibility of ACTN1 to m-calpain cleavage (Sprague et al., 2008). In order to determine if phosphoinositides also enhance the cleavage of ACTN4 by m-calpain, PI(4,5)P2, PI(3,4,5)P3 and PI(3,4)P2 were incubated with ACTN4, respectively at room temperature for 30 min prior to the addition of m-calpain. Contrary to the findings with ACTN1 (Figure 3), all phosphoinositide species inhibited but did not prevent m-calpain cleavage of FL ACTN4 between Tyr13 and Gly14. This suggested that binding of phosphoinositides to ACTN4 is involved in the regulation of ACTN4 cleavage between Tyr13 and Gly14 by m-calpain. Thus, the crosslinking of an ACTN4 dimer to the inner membrane via phosphoinositides may protect this from disruption.

3.4. Binding of ACTN4 to actin filaments in vitro inhibits m-calpain cleavage

ACTN4 crosslinks actin filaments through the binding of its actin binding domain heads residing at both ends of dumbbell shaped anti-parallel ACTN4 homodimer. Our above data shows that m-calpain cuts ACTN4 at its proximal N-terminus that is close to actin binding domain of ACTN4. To determine if binding to actin filaments affects the susceptibility of ACTN4 to m-calpain cleavage, we incubated ACTN4 and G-actin at room temperature in a modified actin binding buffer (which has been optimized to be suitable for both actin binding and m-calpain cleavage) for an hour to allow the formation of ACTN4-actin filaments complex prior to the addition of m-calpain. As shown in Figure 4, binding of WT ACTN4 to actin filaments decreased its susceptibility to cleavage by m-calpain between Tyr 13 and Gly 14. This demonstrates a second level of resistance to dissociation of formed bridges between the cytoskeleton and adhesion plaques.

3.5. The last 11 C-terminal amino acids of ACTN4 are an inhibitory domain for m-calpain cleavage between Lys283 and Val284

While the above suggests a regulatory role for N-terminal cleavage in irreversibly diminishing actin binding, this effect was limited and this action did not mimic other calpain cleavages of separating functional domains. Alpha-actinin consists of three major domains: N-terminal actin binding domain, central rod domain and C-terminal calcium binding motifs, with two monomers forming an anti-parallel dimer (Blanchard et al., 1989). In structurally modeling the ACTN4 homodimer, we found that the C-terminal CaM-like domains appeared to be part of a stable complex that includes the actin binding domain and a neck region which connects the actin binding domain and central rod domain (Travers et al., 2013). To determine whether the calcium binding motifs contribute in protecting the ACTN4 N-terminal from m-calpain cleavage, constructs lacking calcium binding motif 2 (1–841) and motifs 1 & 2 (1–768) were expressed and purified from *E.coli*. Interestingly, a ~ 70 kD fragment readily was produced when both 1–841 and 1–768 were incubated with m-calpain (Figure 5A). N-terminal sequencing analysis revealed that the m-calpain cleavage site of ACTN4 truncated mutant 1–841 and 1–768 was between lysine 283 (Lys283) and valine 284 (Val284). To further confirm that m-calpain cleavage of 1–841 occurred between Lys283 and Val284, Lys283 and Val284 were replaced simultaneously with D and P. Surprisingly, 1–841K283V284/DP was still cleaved by m-calpain resulted in a ~ 70 kD fragment (Figure 5B) suggesting that m-calpain recognition and cleavage sites are conformational dependent rather than strictly based on amino acid sequence. As the removal of either whole calcium binding motif (motifs 1 & 2) or only motif 2 allowed access of m-calpain to a secondary cleavage site Lys283/Val284, we were interested in determining the minimal length of the C-terminal tail which is enough to protect ACTN4 from m-calpain cleavage at this site. Therefore, a series of truncated ACTN4 mutants starting from 860 were constructed by adding 10 amino acids in a coarse scale. As shown in Figure 5C, all truncated

mutants except for 1–900 were almost completely cleaved with m-calpain suggesting that the last 11 amino acids were probably essential to block m-calpain cleavage of ACTN4 between Lys283 and Val284. In order to precisely determine the length of this C-terminal inhibitory tail of ACTN4, another ten truncated mutants were constructed by either removing or adding amino acids one-by-one to 1–900. As shown in Figure 5D, all mutants with size less than 900 residues were almost completely cleaved by m-calpain. In contrast, truncation mutants that were larger than or equal to 900 residues were resistant to m-calpain cleavage between Lys283 and Val284.

In order to determine if the resistance to m-calpain between Lys283 and Val284 due to the last 11 residues of ACTN4 is conserved among non-muscle alpha-actinin isoforms, the same truncations were applied to ACTN1. As shown in Figure 5E, ACTN1 truncated mutants lacking the last 11 or more amino acids (mutant 1–881equals ACTN4 mutant 1–900) were also sensitive to m-calpain cleavage. Taking together, these results suggested that the last 11 amino acids of non-muscle alpha-actinin (isoforms 1 & 4) are essential for inhibiting the cleavage of m-calpain between Lys283 and Val284.

3.6. The C-terminal tail of ACTN4 is essential for maintaining its normal actin binding activity and biological function in migration

Alpha-actinins exist as a functional unit by forming an anti-parallel homodimers through the interaction between the N-terminal actin binding domain of one molecule and the C-terminal calcium binding motifs of another molecule as well as their central rod domains. To test if the removal of C-terminus of ACTN4 affects its actin binding activity, we isolated the cytoskeleton of NR6WT ACTN4 KD fibroblasts transiently expressing either FL WT-ACTN4-eGFP or 1–890 ACTN4-eGFP, a representative of ACTN4 truncation mutant which lacks the C-terminal tail longer than 11 amino acids for the determination of ACTN4 content. Surprisingly, the amount of 1–890-ACTN4-eGFP residing within cytoskeleton was significantly lower compared to full length ACTN4 (Figure 6A).

Of interest, our previous (Shao et al., 2010a) and other studies (Honda et al., 1998, Honda et al., 2005, Kikuchi et al., 2008, Quick and Skalli, 2010, Sen et al., 2009, Yamamoto et al., 2009) had shown that ACTN4 plays an important role in cell migration; we tested the effect of carboxyl tail of ACTN4 on cell migration using a live cell tracking assay. Surprisingly, we found that 1–890 ACTN4-eGFP failed to restore the cell migration of NR6WT ACTN4 KD fibroblasts to NR6WT level in normal growth media while FL WT ACTN4-eGFP fully rescued (Figure 6B). The failure of 1–890 to rescue the cell motility phenotype of ACTN4 KD fibroblasts was not due to its expression level (sum of soluble (S) and cytoskeletal (C), Figure 6A) but was probably due to the increase of its localization in perinuclear cytoplasm which may results in a decreased turnover with actin fiber or other cytoskeleton/membrane proteins and the reduction in its recruitment to the lamellipodial area of moving cells comparing to FL WT ACTN4 (Figure 6C). The function of the c-terminal tail of ACTN4 in cell migration was further confirmed by other truncated ACTN4 mutants (Figure 6D). We had earlier shown that EGF treatment significantly enhances the phosphorylation of ACTN4 at tyrosine 4 (Tyr 4) and tyrosine 31 (Tyr 31) (Shao, Wu, 2010b). To test if the effect of carboxyl terminal of ACTN4 on cell migration is due to the impaired EGF-mediated phosphorylation, we transiently expressed FL WT ACTN4-eGFP and 1–890 ACTN4-eGFP, respectively in NR6WT ACTN4 KD fibroblasts and stimulated cells with 1 nM EGF for 12h after overnight quiescence in 0.1% dialyzed fetal bovine serum (FBS) containing media for continually cell tracking. Interestingly, EGF just slightly enhanced the migration of NR6WT ACTN4 KD fibroblasts in which 1–890ACTN4-eGFP was expressed while the migration of FL WT ACTN4-eGFP expressed fibroblasts were significantly boosted with EGF comparing to non-EGF treatment (Figure 6E). The failure of EGF to stimulate the migration of 1–890 ACTN4-eGFP expressing cells was not due to the effect of truncation on

phosphorylation of ACTN4 at Tyr4 and Tyr31 (Figure 6F). Taken together, these results suggest that the tail of ACTN4 is essential for maintaining its normal actin binding activity and biological function in cell migration.

3.7. The C-terminal tail of ACTN4 is essential for maintaining extent of cell spreading

As a crosslinking protein, ACTN4 has been shown to be essential for maintaining normal cell contactility and thus the extent of spreading of fibroblasts by our previous study (Shao et al., 2010a). To determine if the removal of carboxyl tail of ACTN4 affects its function on cell spreading, we transiently expressed either full length or carboxyl truncated ACTN4-eGFP in NR6WT ACTN4 KD fibroblasts and then reseeded on glass coverslips coated with fibronectin for appropriate time of culture. As shown in Figure 7, full length ACTN4 completely restored the flat cellular cross-sectional area of NR6WT ACTN4 KD fibroblasts to the size of NR6WT fibroblasts. However, both 1–890 and 1–841 failed to rescue the flat size of cellular cross-sectional area of NR6WT ACTN4 KD fibroblasts suggesting that the carboxyl tail of ACTN4 is essential for its normal function in cell spreading.

4. Discussion

Sprague et al. (Sprague et al., 2008) showed that both native chicken gizzard ACTN1 and its actin binding domain which was fused to GST, expressed and purified from *E. coli* were cleaved by m-calpain between Y246 and H247 *in vitro* and their susceptibility to m-calpain were significantly enhanced by the binding to phosphoinositides PI(3,4,5)P3 although alpha-actinin was previously suggested to not be a good substrate of m-calpain *in vitro* (Beckerle et al., 1987). Our results show that m-calpain cleaves ACTN4 between Tyr13 and Gly14 and the truncated large fragment 14–911 is resistant to higher concentration of m-calpain up to 200 μM. This is no surprise as ACTN4 has an extra N-terminus with a length of 19 amino acids which includes the m-calpain cleavage site Tyr13-Gly14 which is absent in ACTN1. We detected only a minor population of cleaved ACTN4 in cells (Figure 1G). This is consistent with two aspects. First, the binding of ACTN4 to actin filaments and phosphoinositides which have been confirmed by our *in vitro* studies, as well as the binding to focal adhesion proteins, likely limits cleavage. Second, we also found that EGF-stimulated phosphorylation of ACTN4 at Tyr4 and Tyr31 slightly inhibited its cleavage by m-calpain between Tyr13 and Gly14 (data not shown). And lastly, intracellular calpains by and large act as substoichiometric ‘clippases’ that generate persistent functional protein domains (Glading et al., 2002). Although only a minor fraction of ACTN4 is cleaved by m-calpain, it may be sufficient for its cellular and biological function. Our previous studies also showed that the EGF-mediated phosphorylation of ACTN4 is much stronger than ACTN1 at Y4 of ACTN4, a major phosphorylation site which is absent in ACTN1 and Y31, a minor phosphorylation site which equates to ACTN1 Y12, a phosphorylation site for focal adhesion kinase (FAK) (Izaguirre et al., 2001, Shao et al., 2010b). Previous studies and our present study that ACTN4 c-terminal truncated mutants fail to restore cell migration and spreading of ACTN4 KD fibroblasts to level of wild type cells in which ACTN1 is normally expressed suggest that ACTN1 and ACTN4 play distinct biological roles although they share 86 percent sequence identity.

Our live cell tracking experiment revealed that ACTN4 KD fibroblasts transiently expressing 14–911, a large fragment representing m-calpain cleaved ACTN4, migrate with less persistence comparing to FL WT ACTN4 expressed ACTN4 KD fibroblasts. This helps us understand why m-calpain cleavage of ACTN4 between Tyr13 and Gly14 is partially inhibited by binding to either phosphoinositides or actin filaments. For example, in addition to bundling actin filaments, ACTN4 links actin filaments to cellular membrane where vinculin, talin, integrins, membrane receptors and phosphoinositides such as PI(4,5)P2 and PI(3,4,5)P3 majorly localize (Fukami et al., 1992, Ziegler et al., 2008). Once ACTN4 binds

to phosphoinositides it becomes less susceptible to m-calpain resulting in an enhancement of its phosphorylation, after stimulation by EGF or other growth factors. On the other hand, although the cleavage of ACTN4 between Tyr13 and Gly14 by m-calpain results in a loss of Y4, a major site for EGF-mediated phosphorylation of ACTN4 and does not affect the binding of 14–911 to actin filaments, this cleavage is probably essential for preventing ACTN4 from EGF-mediated phosphorylation at Y4 which results in a decrease in its actin binding activity when its normal activity is required.

To date, accumulating evidence suggest that ACTN4 functions as a key player in cell motility, cancer metastasis and kidney failure besides actin crosslinking (Honda et al., 1998, Honda et al., 2005, Kikuchi et al., 2008, Kos et al., 2003, Michaud et al., 2003, Shao et al., 2010a). The crystal structures of distinct alpha-actinin domains have been resolved and their precise functions are being gradually deciphered. The C-terminus of ACTN4 consists of calcium binding motifs which have been shown not only to be essential for the inhibition of its binding affinity for actin filaments by calcium but also to be involved in formation of a ternary complex (Travers et al., 2013), as well as the interaction between two molecules of actinin dumbbell shaped homodimer. In this study, we find that removal of the ACTN4 C-terminal tail dramatically enhances susceptibility of a secondary site Lys283–Val284 to m-calpain cleavage due to unbinding of the neck region containing the target site from CaM2. Interestingly, truncation of c-terminal tail of ACTN4 significantly causes retention in cytoplasm and thus a dramatic reduction at the lamellipodial area of a moving cell where most of full length wild type ACTN4 accumulate (Figure 6C). This is probably due to its impaired actin binding activity (Figure 6A) as the inhibition of actin bundling activity of ACTN4 by MTBP significantly decreases the filopodia formation which results in a reduction in the cell motility of both human osteosarcoma and wild type cell lines (Agarwal et al., 2013).

Our findings for the first time show that ACTN4 is a substrate of m-calpain and this cleavage is regulated by its binding to phosphoinositides and actin filaments. Cleavage of ACTN4 by m-calpain between Tyr13 and Gly14 impairs its function in maintaining the directional persistence during cellular migration. Besides the role of ACTN4 in cross-linking actin filaments, it also plays important roles in the maturation of focal adhesion by recruiting focal adhesion related proteins to form a complex at focal adhesion sites. Therefore, further investigations focusing on how m-calpain cleavage regulates the function of ACTN4 in the dynamic modeling of cytoskeleton and the maturation of focal adhesion need to be next addressed. Furthermore, the molecular mechanisms by which truncation of the C-terminal of ACTN4 affects its function in cell motility and spreading and how the removal of N-terminal disordered domain impairs cell migratory persistence await further investigaions.

Acknowledgments

We thank the Center of Biological Images at University of Pittsburgh for providing fluorescent microscopy. This project is supported by grants from National Institutes of Health’s National Institute for General Medical Sciences.

References

Agarwal N, Adhikari AS, Iyer SV, Hekmatdoost K, Welch DR, Iwakuma T. MTBP suppresses cell migration and filopodia formation by inhibiting ACTN4. Oncogene. 2013; 32:462–470. [PubMed: 22370640]

Beckerle MC, Burridge K, DeMartino GN, Croall DE. Colocalization of calcium-dependent protease II and one of its substrates at sites of cell adhesion. Cell. 1987; 51:569–577. [PubMed: 2824061]

Blanchard A, Ohanian V, Critchley D. The structure and function of alpha-actinin. J Muscle Res Cell Motil. 1989; 10:280–289. [PubMed: 2671039]

Borrego-Diaz E, Kerff F, Lee SH, Ferron F, Li Y, Dominguez R. Crystal structure of the actin-binding domain of alpha-actinin 1: evaluating two competing actin-binding models. J Struct Biol. 2006; 155:230–238. [PubMed: 16698282]

Chou J, Stolz DB, Burke NA, Watkins SC, Wells A. Distribution of gelsolin and phosphoinositol 4,5-bisphosphate in lamellipodia during EGF-induced motility. Int J Biochem Cell Biol. 2002; 34:776–790. [PubMed: 11950594]

Davison MD, Critchley DR. alpha-Actinins and the DMD protein contain spectrin-like repeats. Cell. 1988; 52:159–160. [PubMed: 3342446]

Dourdin N, Bhatt AK, Dutt P, Greer PA, Arthur JS, Elce JS, et al. Reduced cell migration and disruption of the actin cytoskeleton in calpain-deficient embryonic fibroblasts. J Biol Chem. 2001; 276:48382–48388. [PubMed: 11602605]

Fukami K, Furuhashi K, Inagaki M, Endo T, Hatano S, Takenawa T. Requirement of phosphatidylinositol 4,5-bisphosphate for alpha-actinin function. Nature. 1992; 359:150–152. [PubMed: 1326084]

Glading A, Lauffenburger DA, Wells A. Cutting to the chase: calpain proteases in cell motility. Trends Cell Biol. 2002; 12:46–54. [PubMed: 11854009]

Glading A, Uberall F, Keyse SM, Lauffenburger DA, Wells A. Membrane proximal ERK signaling is required for M-calpain activation downstream of epidermal growth factor receptor signaling. J Biol Chem. 2001; 276:23341–23348. [PubMed: 11319218]

Honda K, Yamada T, Endo R, Ino Y, Gotoh M, Tsuda H, et al. Actinin-4, a novel actin-bundling protein associated with cell motility and cancer invasion. J Cell Biol. 1998; 140:1383–1393. [PubMed: 9508771]

Honda K, Yamada T, Hayashida Y, Idogawa M, Sato S, Hasegawa F, et al. Actinin-4 increases cell motility and promotes lymph node metastasis of colorectal cancer. Gastroent. 2005; 128:51–62.

Izaguirre G, Aguirre L, Hu YP, Lee HY, Schlaepfer DD, Aneskievich BJ, et al. The cytoskeletal/non-muscle isoform of alpha-actinin is phosphorylated on its actin-binding domain by the focal adhesion kinase. J Biol Chem. 2001; 276:28676–28685. [PubMed: 11369769]

Kikuchi S, Honda K, Tsuda H, Hiraoka N, Imoto I, Kosuge T, et al. Expression and gene amplification of actinin-4 in invasive ductal carcinoma of the pancreas. Clin Cancer Res. 2008; 14:5348–5356. [PubMed: 18765526]

Kos CH, Le TC, Sinha S, Henderson JM, Kim SH, Sugimoto H, et al. Mice deficient in alpha-actinin-4 have severe glomerular disease. J Clin Invest. 2003; 111:1683–1690. [PubMed: 12782671]

Lee SH, Weins A, Hayes DB, Pollak MR, Dominguez R. Crystal structure of the actin-binding domain of alpha-actinin-4 Lys255Glu mutant implicated in focal segmental glomerulosclerosis. J Mol Biol. 2008; 376:317–324. [PubMed: 18164029]

Leloup L, Shao H, Bae YH, Deasy B, Stolz D, Roy P, et al. m-Calpain activation is regulated by its membrane localization and by its binding to phosphatidylinositol 4,5-bisphosphate. J Biol Chem. 2010; 285:33549–33566. [PubMed: 20729206]

Michaud JL, Hosseini-Abardeh M, Farah K, Kennedy CR. Modulating alpha-actinin-4 dynamics in podocytes. Cell Motil Cytoskel. 2009; 66:166–178.

Michaud JL, Lemieux LI, Dube M, Vanderhyden BC, Robertson SJ, Kennedy CR. Focal and segmental glomerulosclerosis in mice with podocyte-specific expression of mutant alpha-actinin-4. J Am Soc Nephrol. 2003; 14:1200–1211. [PubMed: 12707390]

Ono Y, Sorimachi H. Calpains: an elaborate proteolytic system. Biochim Biophys Acta. 2012; 1824:224–236. [PubMed: 21864727]

Otey CA, Carpen O. Alpha-actinin revisited: a fresh look at an old player. Cell Motil Cytoskel. 2004; 58:104–111.

Otto JJ. Actin-bundling proteins. Curr Opin Cell Biol. 1994; 6:105–109. [PubMed: 8167015]

Quick Q, Skalli O. Alpha-actinin 1 and alpha-actinin 4: contrasting roles in the survival, motility, and RhoA signaling of astrocytoma cells. Exp Cell Res. 2010; 316:1137–1147. [PubMed: 20156433]

Schoenwaelder SM, Kulkarni S, Salem HH, Imajoh-Ohmi S, Yamao-Harigaya W, Saido TC, et al. Distinct substrate specificities and functional roles for the 78- and 76-kDa forms of mu-calpain in human platelets. J Biol Chem. 1997; 272:24876–24884. [PubMed: 9312088]

Sen S, Dong M, Kumar S. Isoform-specific contributions of alpha-actinin to glioma cell mechanobiology. PLoS One. 2009; 4:e8427. [PubMed: 20037648]

Shao H, Chou J, Baty CJ, Burke NA, Watkins SC, Stolz DB, et al. Spatial localization of m-calpain to the plasma membrane by phosphoinositide biphosphate binding during epidermal growth factor receptor-mediated activation. Mol Cell Biol. 2006; 26:5481–5496. [PubMed: 16809781]

Shao H, Wang JH, Pollak MR, Wells A. alpha-actinin-4 is essential for maintaining the spreading, motility and contractility of fibroblasts. PLoS One. 2010a; 5:e13921. [PubMed: 21085685]

Shao H, Wu C, Wells A. Phosphorylation of alpha-actinin 4 upon epidermal growth factor exposure regulates its interaction with actin. J Biol Chem. 2010b; 285:2591–2600. [PubMed: 19920151]

Sjoblom B, Salmazo A, Djinovic-Carugo K. Alpha-actinin structure and regulation. Cell Molec Life Sci. 2008; 65:2688–2701. [PubMed: 18488141]

Sprague CR, Fraley TS, Jang HS, Lal S, Greenwood JA. Phosphoinositide binding to the substrate regulates susceptibility to proteolysis by calpain. J Biol Chem. 2008; 283:9217–9223. [PubMed: 18258589]

Tompa P, Buzder-Lantos P, Tantos A, Farkas A, Szilagyi A, Banoczi Z, et al. On the sequential determinants of calpain cleavage. J Biol Chem. 2004; 279:20775–20785. [PubMed: 14988399]

Travers T, Shao H, Wells A, Camacho C. Towards a cogent quantitative model of the regulatory network of α-actinin-4 and actin interactions. Biophys J. 2013 In Press.

Weins A, Schlondorff JS, Nakamura F, Denker BM, Hartwig JH, Stossel TP, et al. Disease-associated mutant alpha-actinin-4 reveals a mechanism for regulating its F-actin-binding affinity. Proc Natl Acad Sci U S A. 2007; 104:16080–16085. [PubMed: 17901210]

Xie H, Pallero MA, Gupta K, Chang P, Ware MF, Witke W, et al. EGF receptor regulation of cell motility: EGF induces disassembly of focal adhesions independently of the motility-associated PLCgamma signaling pathway. J Cell Sci. 1998; 111(Pt 5):615–624. [PubMed: 9454735]

Yamamoto S, Tsuda H, Honda K, Onozato K, Takano M, Tamai S, et al. Actinin-4 gene amplification in ovarian cancer: a candidate oncogene associated with poor patient prognosis and tumor chemoresistance. Mod Pathol. 2009; 22:499–507. [PubMed: 19151661]

Ylanne J, Scheffzek K, Young P, Saraste M. Crystal structure of the alpha-actinin rod reveals an extensive torsional twist. Structure. 2001; 9:597–604. [PubMed: 11470434]

Ziegler WH, Gingras AR, Critchley DR, Emsley J. Integrin connections to the cytoskeleton through talin and vinculin. Biochem Soc Trans. 2008; 36:235–239. [PubMed: 18363566]

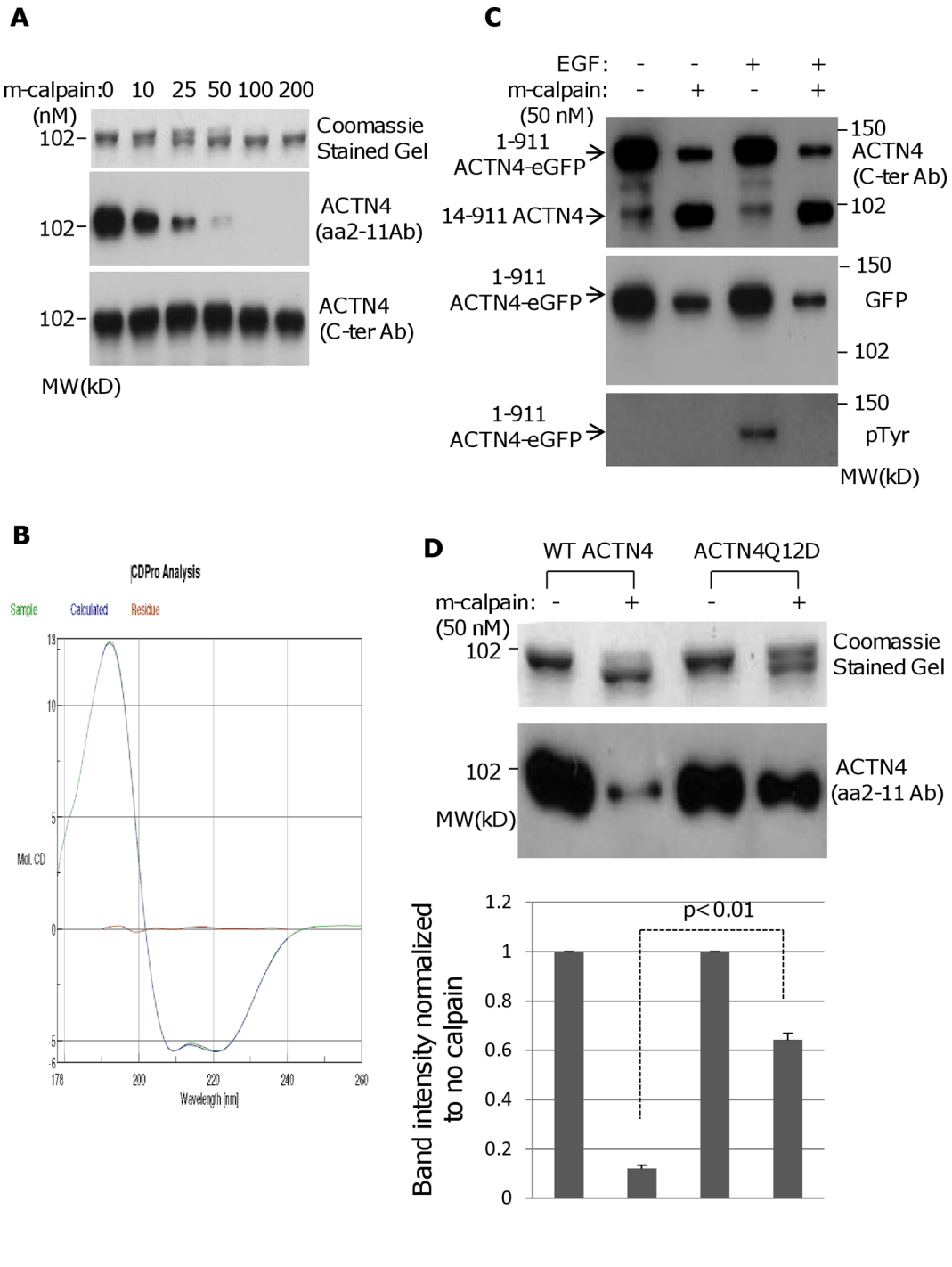

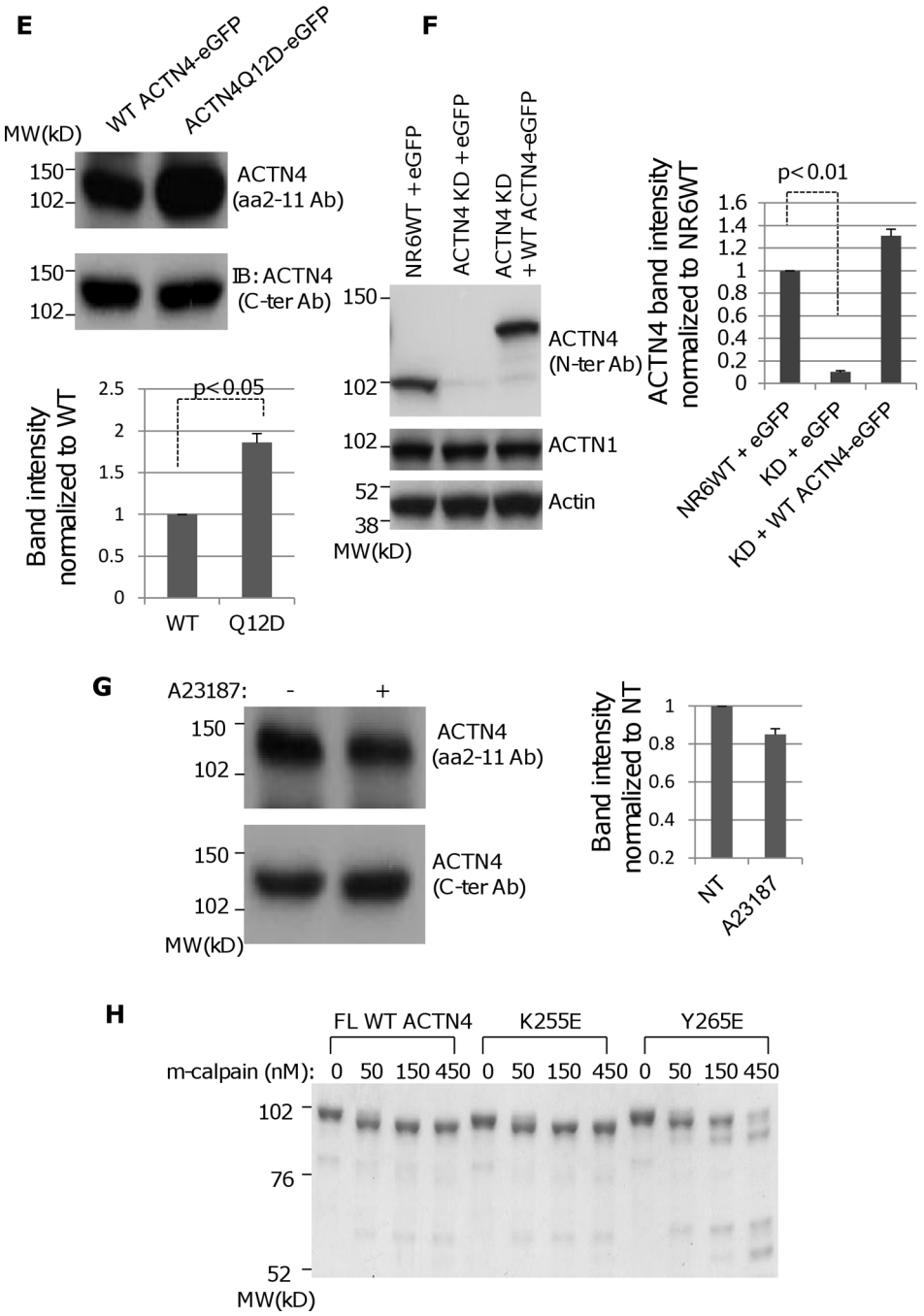

Fig. 1.

m-Calpain cleaves ACTN4. (A) Full length WT ACTN4 expressed and purified in *E.Coli* were digested with indicated amount of rat m-calpain and separated by SDS-PAGE followed by either staining with Coomassie (top panel) or immunoblotting using ACTN4 antibody aa 2–11 (middle panel) and C-ter (bottom pane). (B) Graphic of circular dichroism. (C) NR6WT ACTN4 KD fibroblasts transiently expresseing FL WT ACTN4-eGFP were starved in quiescence media for 18h prior to treatment with 10 nM EGF for 15 min followed by immunoprecipitation against GFP. Immunoprecipitated protein was digested with m-calpian and then separated by SDS-PAGE followed by immunoblotting using indicated antibodies. (D) m-calpain cleavage of both FL WT ACTN4 and ACTN4 mutant Q12D. Top panel:

Coomassied stained gel; Bottom panel: immunoblotting for ACTN4 using aa 2–11 antibody. The densitometry results for the FL ACTN4 immunoblotting normalized to no m-calpain are shown. (E) Both FL WT ACTN4-eGFP and ACTN4Q12D-eGFP were transiently expressed in NR6WT ACTN4 KD fibroblasts. The total cell lysate was separated by SDS-PAGE followed by immunoblotting using aa 2–11 (top panel) and C-ter antibodies (bottom panel). The densitometry results for the FL ACTN4Q12D immunoblotting normalized to FL WT ACTN4 are shown. (F) Immunoblottings of indicating protein expressed in fibroblasts. (G) Immunoblottings of FL WT ACTN4-eGFP in NR6WT ACTN4 KD fibroblasts w/wo A23187 (10uM) treatment. The densitometry results for the FL ACTN4 immunoblotting normalized to no A23187 treatment are shown. (H) Coomassie stained gel of m-calpain digested FL WT and mutant ACTN4 expressed and purified in *E.coli*. Images represent one of three independent experiments.

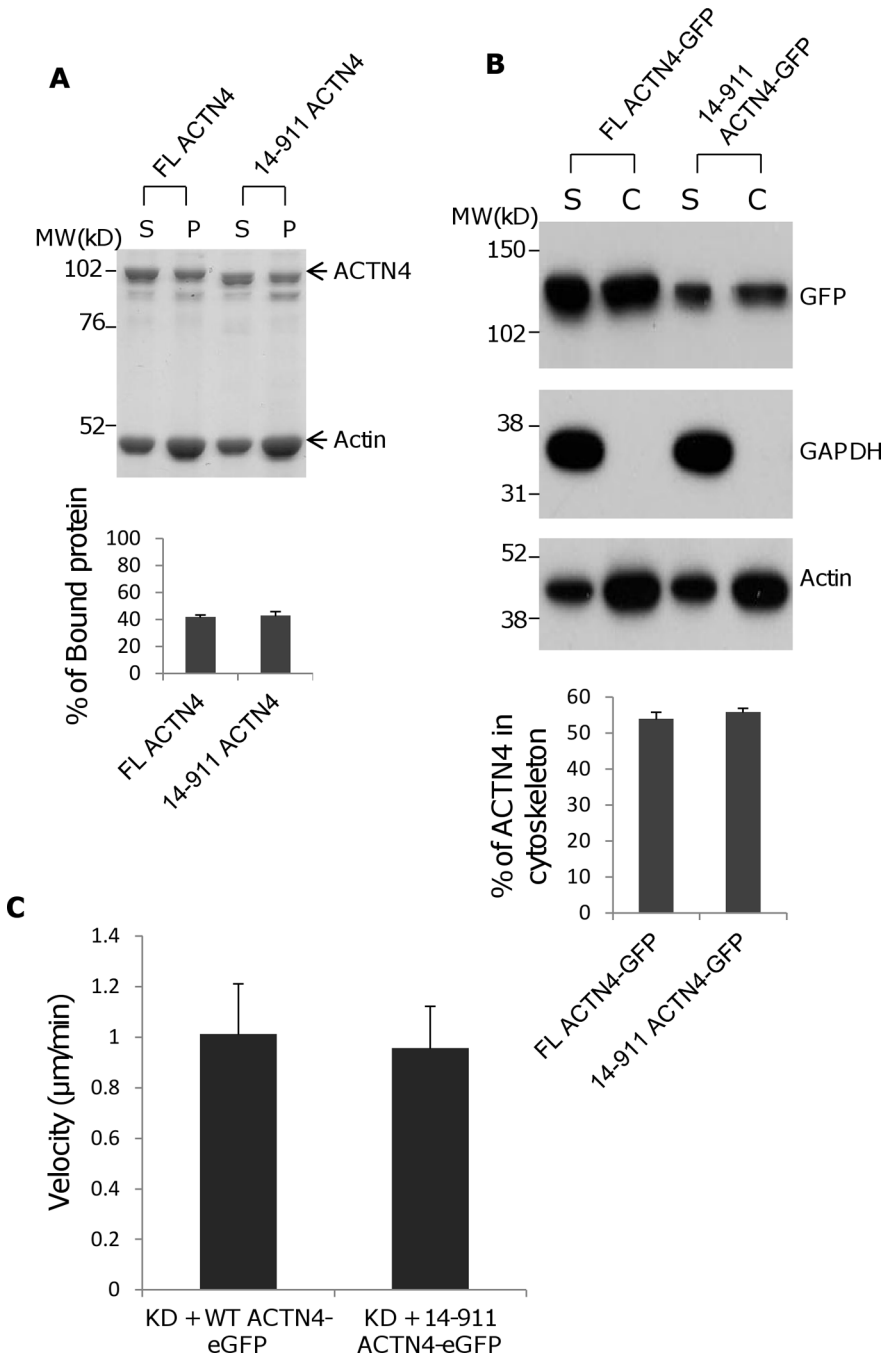

D

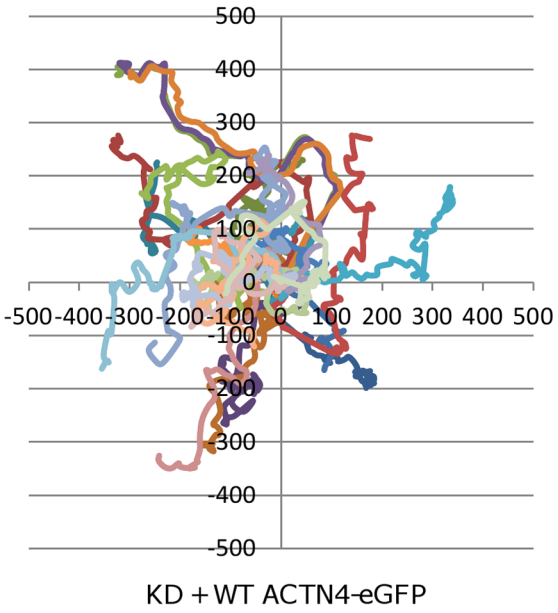

KD + WT ACTN4-eGFP

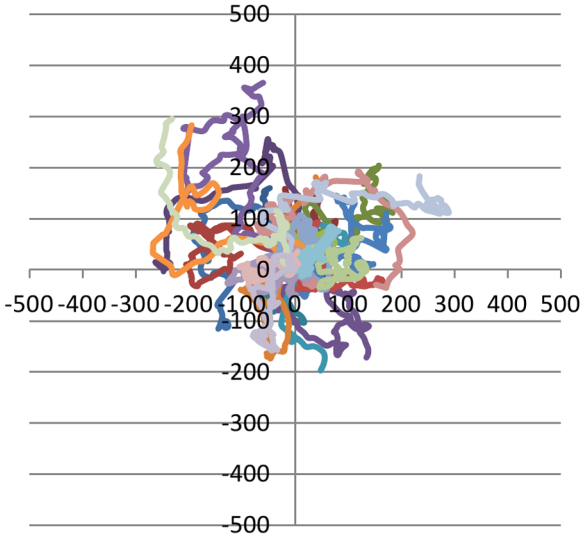

KD + 14-911 ACTN4-eGFP

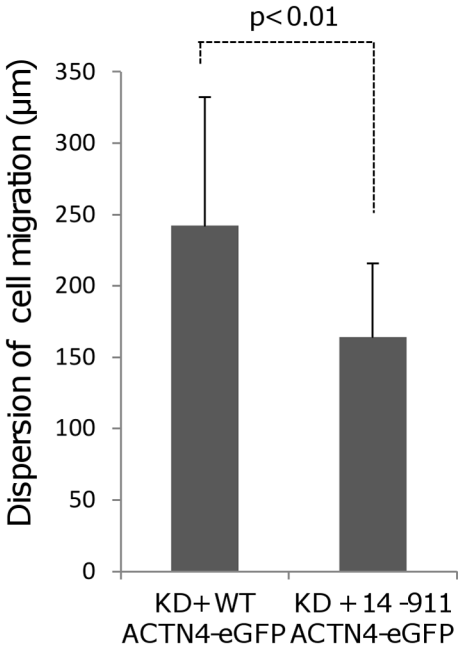

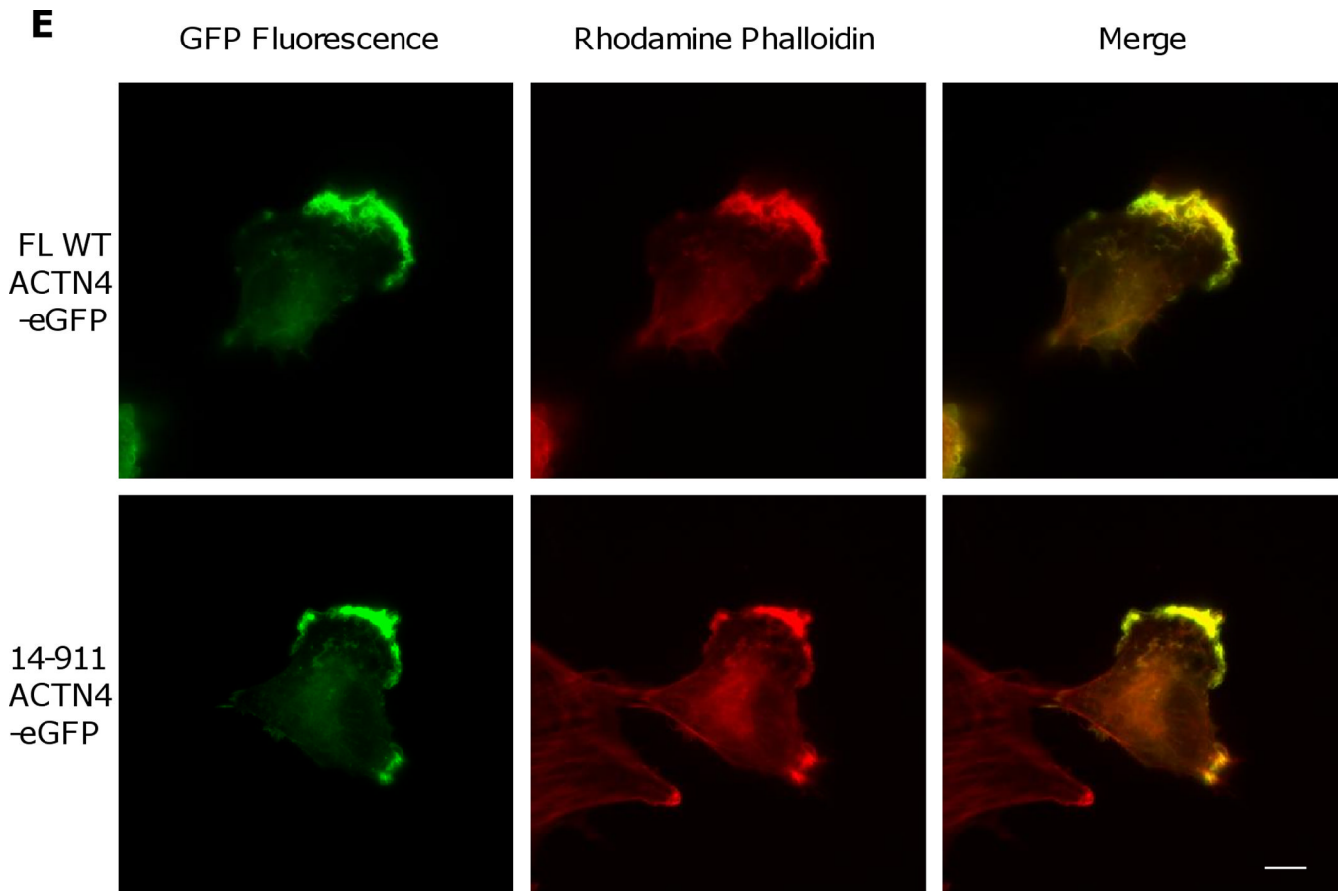

Fig. 2.

Actin binding activity of 14–911 and its effects on cell migration. (A)WT ACTN4 and its truncated fragment 14–911 expressed and purified in *E.Coli* and dialyzed completely against actin binding buffer were incubated with G-actin in actin binding buffer at room temperature for 1h. F-actin and bound ACTN4 were pulled down by centrifugation at 100,000 × g for 30 min at 25 °C. Equal amounts of supernatant and pellets were loaded and separated by polyacrylamide gel followed by Coomassie staining and quantified using Image J software and represented by graph. “S” stands for supernatant and “P” stands for pellet. Image analysis and quantitation of three independent experiments are shown. (B) Immunoblotting of soluble and cytoskeletal ACTN4. See methods for the isolation of cytoskeleton. Quantification presents the amount of ACTN4 in cytoskeleton. The densitometry results for the ACTN4-eGFP immunoblotting are shown. (C) Live cell tracking of NR6WT ACTN4 knockdown (KD) fibroblasts transiently transfected with indicated ACTN4 plasmids. Live cell tracking of transfected cell grown in complete growth media were performed under Nikon live fluorescent microscopy for 16h. Cell migration speed was analyzed using Metamorph software, n=30. Quantitative results represent at least three independent experiments. (D) Trace and dispersion of cell migration of NR6WT ACTN4 KD fibroblasts transiently expressing WT ACTN4-eGFP and 14–911 ACTN4-eGFP, respectively. Lines are created using Metamorph software, n=20. (E) NR6WT ACTN4 KD fibroblasts transiently expressing WT ACTN4-eGFP or 14–911 ACTN4-eGFP were fixed, permeabilized and then stained with rhodamine phalloidin. *Scale bar = 5 μm*. Shown are representative images of at least three experiments.

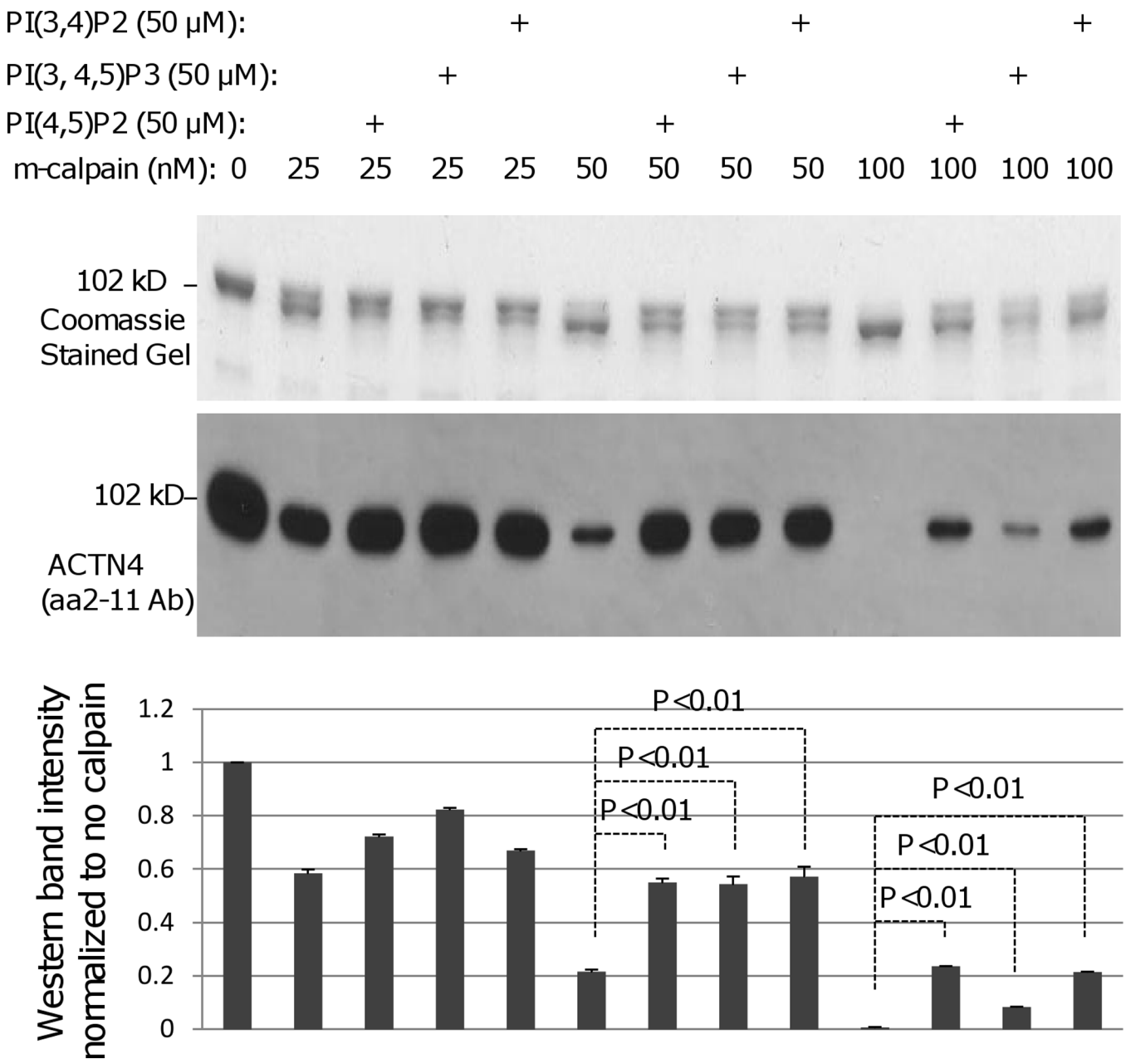

Fig. 3.

Phophoinositides inhbit the cleavage of WT ACTN4 by m-calpain between Y13 and G14. Phosphoinositides PI(4,5)P2, PI(3,4,5)P3, or PI(3,4) (50 μM each) were incubated with ACTN4 at room temperature for 30 min prior to the incubation with indicated amount of m-calpain for additional 1h at 30°C. Reaction was stopped by the addition of 1/5 reaction volume of 5× SDS sample buffer followed by 3 min boiling to denature proteins. Protein bands were separated by SDS-PAGE followed by either staining with Coomassie or immunoblotting of ACTN4 antibody aa 2–11. Graph represents the density of each band of aa 2–11 immunoblotting. Image represents one of three independent experiments.

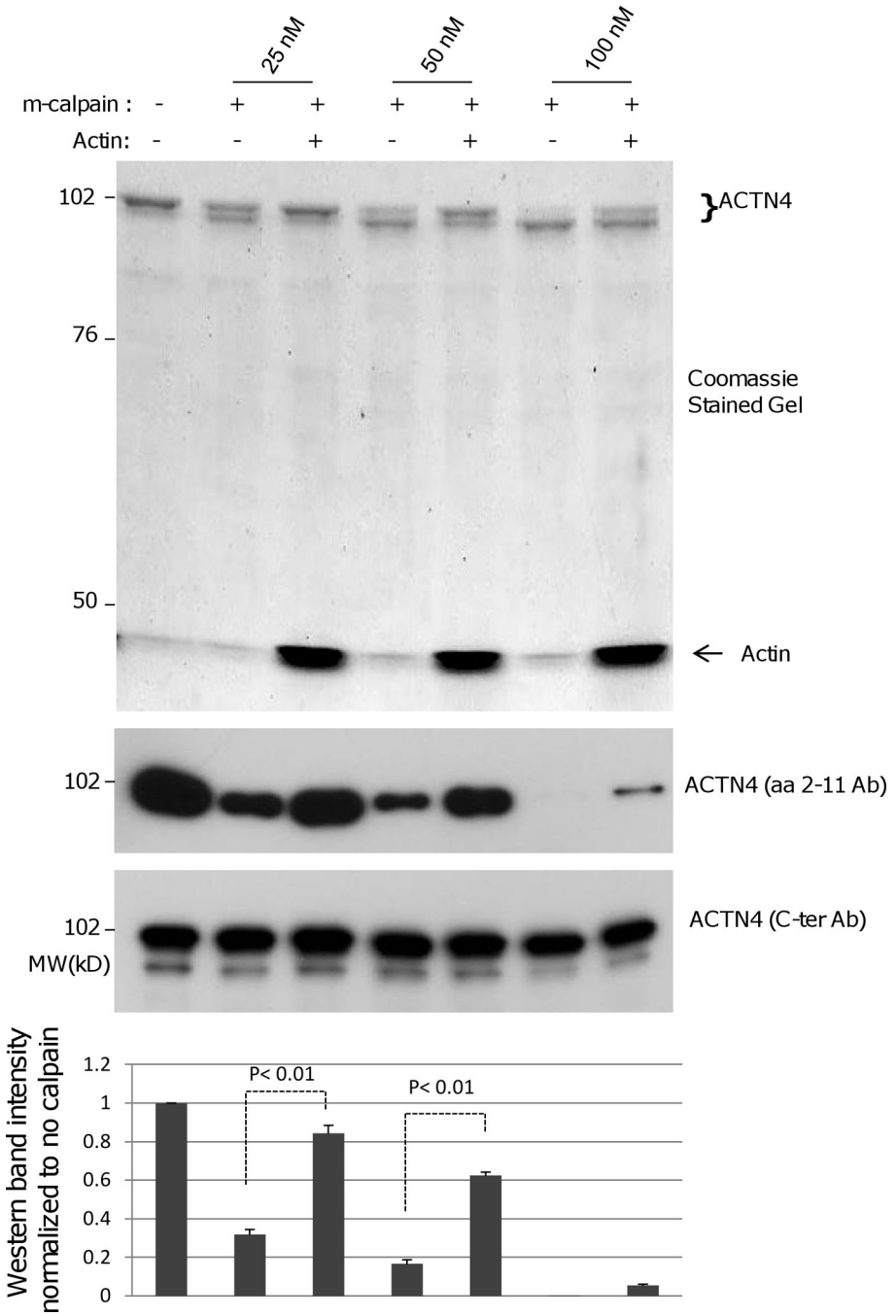

Fig. 4.

Binding to actin filaments inhibits the m-calpain cleavage of WT ACTN4 between Y13 and G14. Pure FL WT and 1–768 ACTN4 were incubated with mono-actin in the presence of 0.5 mM ATP at room temperature for 1h prior to the addition of indicating amount of m-calpain for further incubation at 30 °C for 1h. Reaction was stopped by addition of 1/5 reaction volume of 5× SDS sample buffer followed by 3 min boiling to denature proteins. Protein bands were separated by SDS-PAGE followed by Coomassie staining (up panel) or immunoblotting using ACTN4 antibody aa 2–11(middle panel) and C-ter (bottom pane). Graph represents the density of each band of aa 2–11 immunoblotting. Image represents one of three independent experiments.

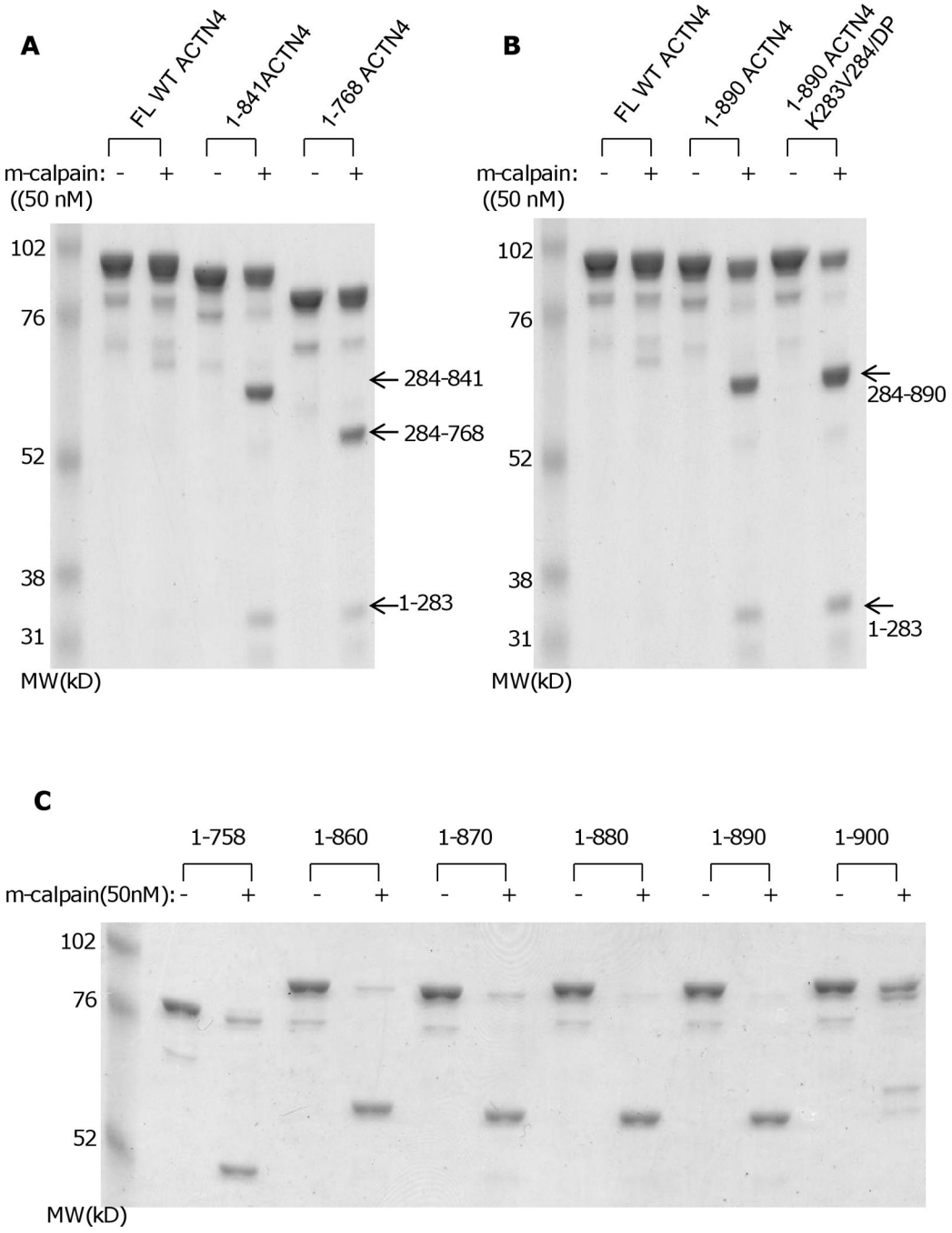

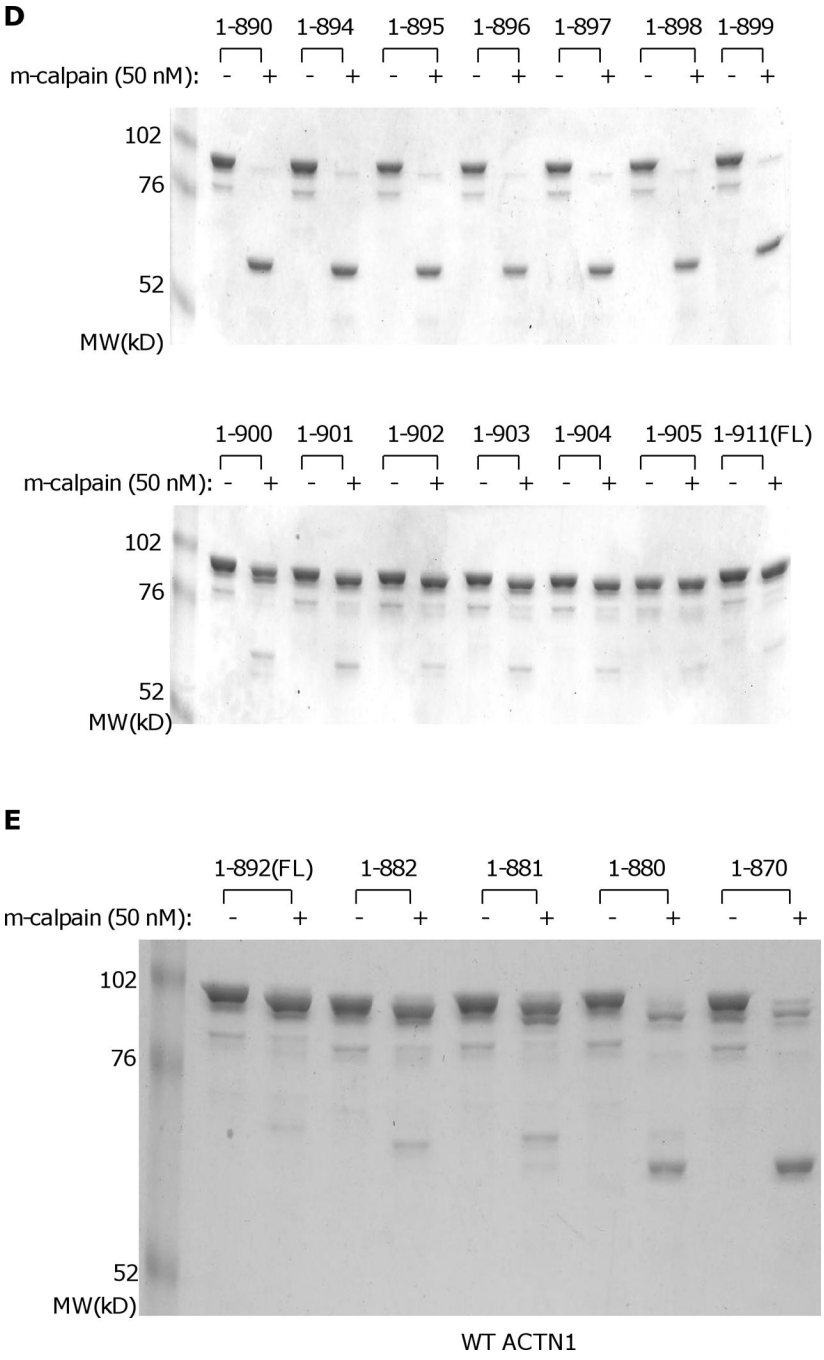

Fig. 5.

Truncation of the C-terminal tail of ACTN4 alters its susceptibility to m-calpain cleavage. Purified protein was digested with m-calpain and bands were separated by SDS-PAGE. Image represents one of three independent experiments. (A) FL WT ACTN4 and 1–768 ACTN4; (B) FL WT ACTN4 and ACTN4 mutants with C-terminal truncation w/wo substitute of secondary m-calpain cleavage site; (C and D) ACTN4 mutants with different length of C-terminal truncation; (E) FL WT ACTN1 and its mutants with different length of C-terminal truncation.

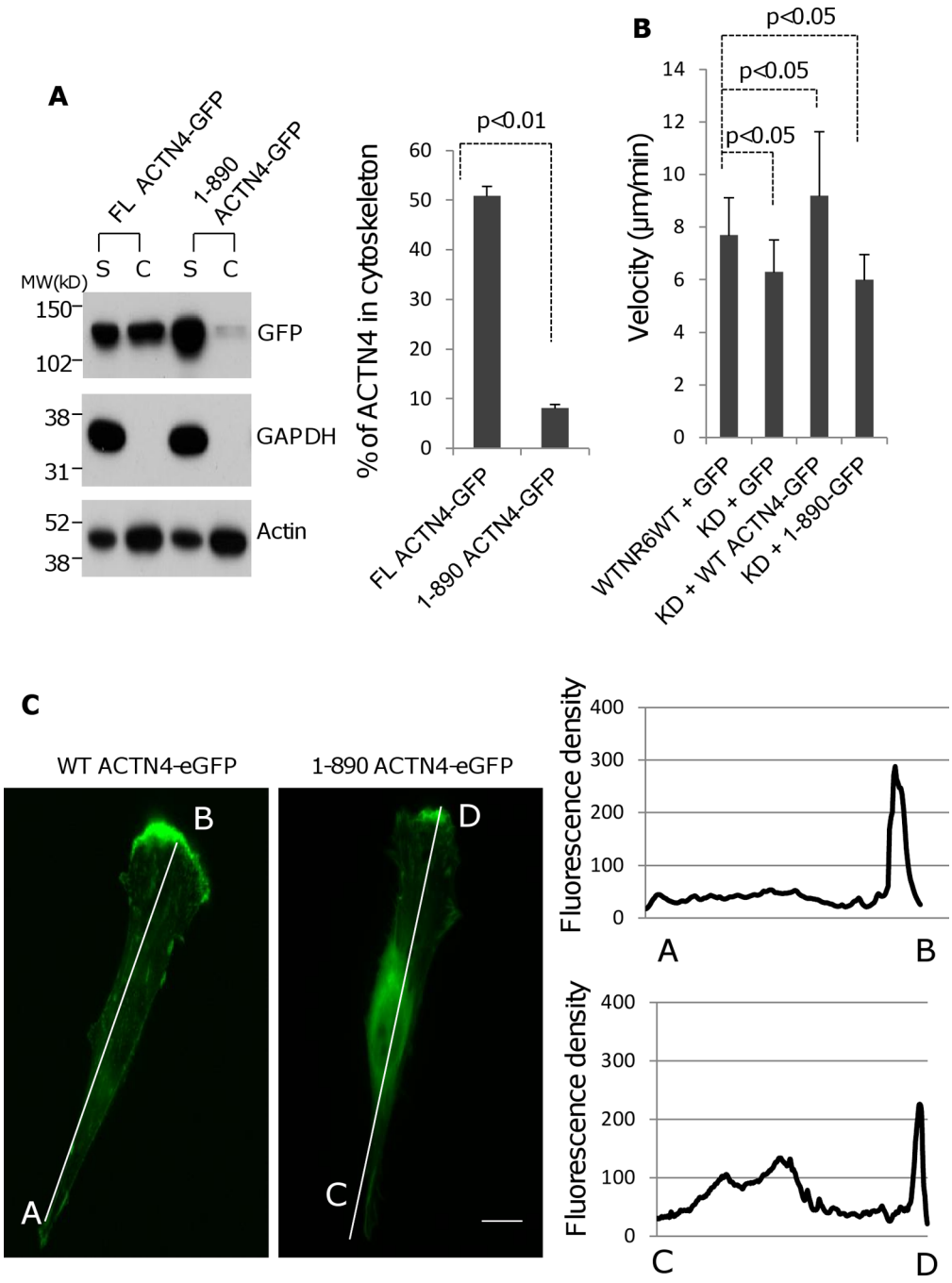

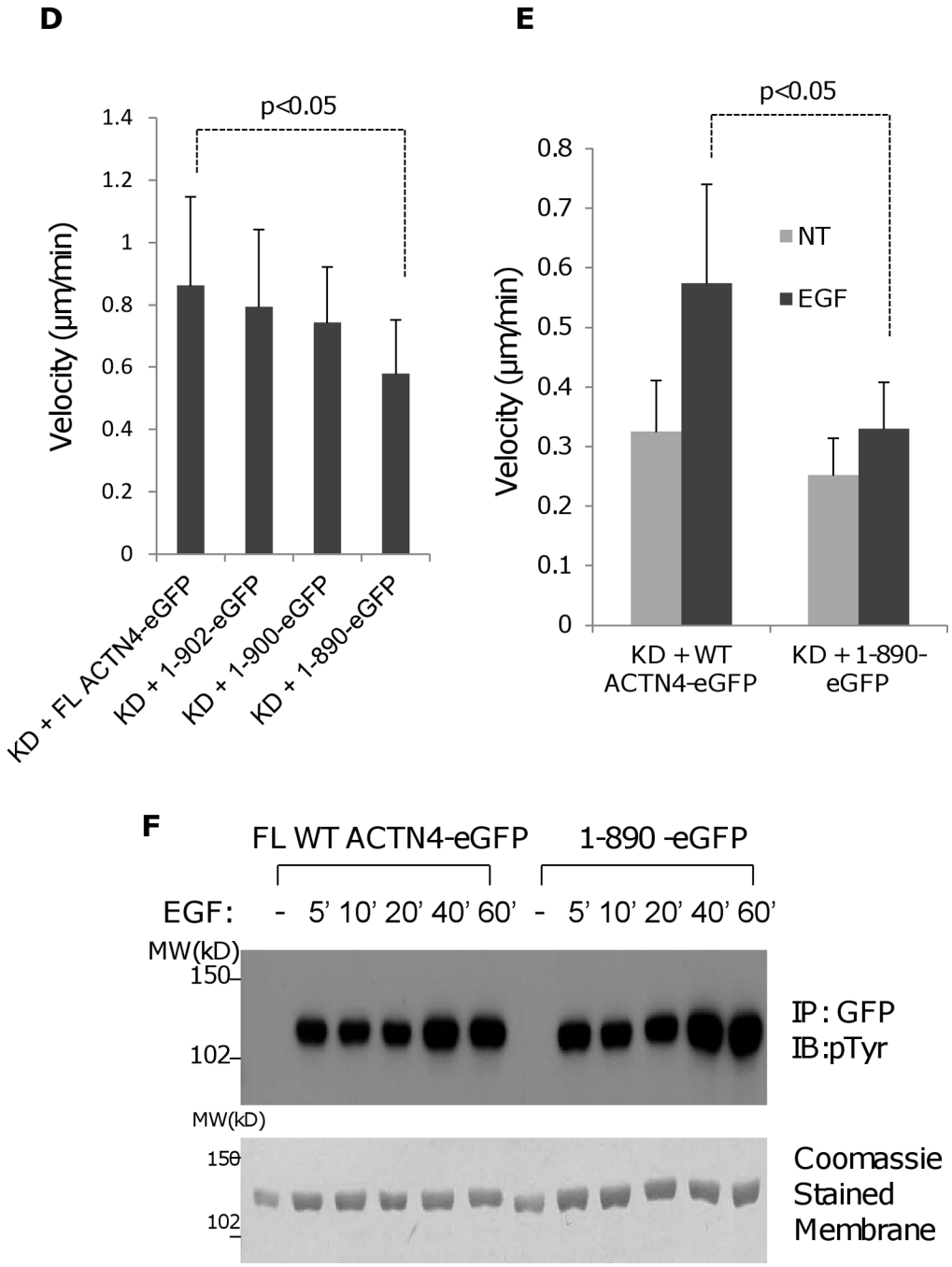

Fig. 6.

Truncation of ACTN4 C-terminal tail affects its actin binding activity and function in cell migration. (A) Immunoblotting of soluble and cytoskeletal ACTN4.. Quantification presents the amount of ACTN4 in cytoskeleton. (B) Live cell tracking of NR6WT ACTN4 knockdown (KD) fibroblasts transiently transfected with indicated ACTN4 plasmids in normal growth media. Live cell tracking of transfected cell grown in complete growth media were performed under Nikon live fluorescent microscopy for 16h. Cell migration speed was analyzed using Metamorph software, n=30. (C) Representative images of expression of WT ACTN4-eGFP and 1–890 ACTN4-eGFP in NR6WT ACTN4 KD fibroblasts (above panel) and their scans of fluorescent density along white line A towards B (WT) and C towards D

(1–890) (bottom graphs). *Scale bar = 5 μm*. (D and E) Live cell tracking of NR6WT ACTN4 knockdown (KD) fibroblasts transiently transfected with indicated ACTN4 plasmids in normal growth media (D) or quiescence media containing 0.1% dialysed FBS (E) for 16h. Cell migration speed was analyzed using Metamorph software, n=30. (F) Immunoblotting of phosphorylated ACTN4 at tyrosines. NR6WT ACTN4 KD fibroblasts expressing WT ACTN4-eGFP or 1–890ACTN4-eGFP were quiesced with quiescence media containing 0.1% dialyzed FBS for 16 h prior to an addition 100 μM of vanadate for further 30 min incubation. After stimulation of 10 nM EGF for 10 min, cells were washed once with cold PBS and then lysed with RIPA buffer containing 1 × protease inhibitors mixture. ACTN4 proteins were purified by immunoprecipitation (IP) against monoclonal GFP antibody and separated by SDS-PAGE and then immunoblotted (IB) with phosphotyrosine (pTyr) antibody (upper panel). Total protein transferred to PVDF membrane was stained with Coomassie Blue G-250 (lower panel). NT, no treatment. Shown are representative of three independent experiments. All quantitative results above represent at least three independent experiments. $P < 0.05$.

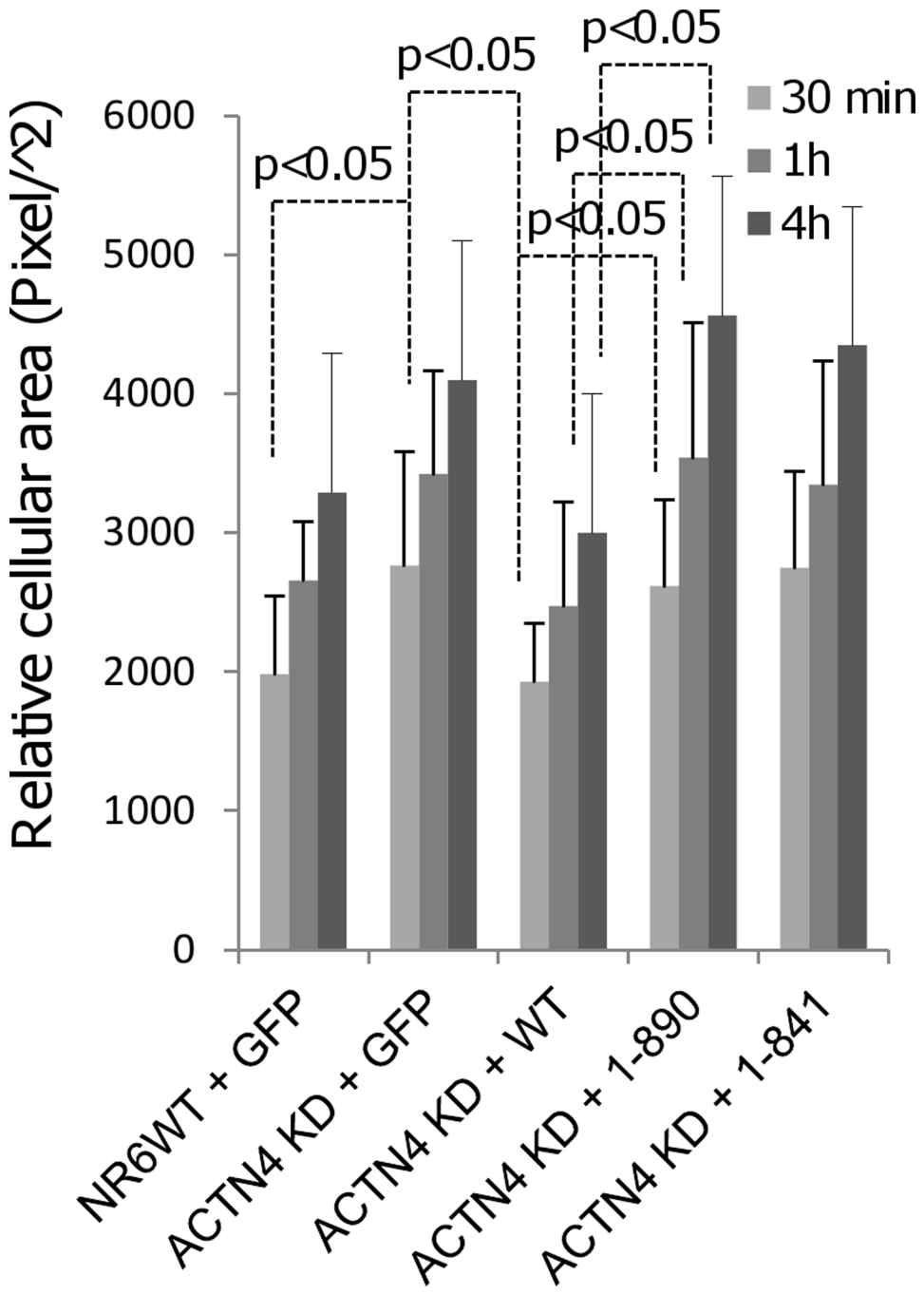

Fig. 7.

Truncation of the C-terminal tail of ACTN4 alters its function in cell spreading. NR6WT Experimental procedure is described in “method”. Quantification represents the average cellular cross-sectional area of at least 100 individual fluorescent cells chosen randomly. Error bars are means ± s.d.. $P < 0.05$.